EPJ AP

Applied Physics

EPJ.org

your physics journal

Eur. Phys. J. Appl. Phys. (2013) 61: 30803 DOI: 10.1051/epjap/2013120172

Analysis of current density and electric field beneath a bipolar DC wires-to-plane corona discharge in humid air

Massinissa Aissou, Hakim Aitsaid, Hamou Nouri, and Youcef Zebboudj

edp sciences

The title “The European Physical Journal” is a joint property of EDP Sciences, Società Italiana di Fisica (SIF) and Springer

Eur. Phys. J. Appl. Phys. (2013) 61: 30803
DOI: 10.1051/epjap/2013120172

THE EUROPEAN PHYSICAL JOURNAL
APPLIED PHYSICS

Regular Article

Analysis of current density and electric field beneath a bipolar DC wires-to-plane corona discharge in humid air

Massinissa Aissou, Hakim Aitsaid, Hamou Nouri, and Youcef Zebboudj[a]

Laboratoire de Génie Electrique, Université A. Mira de Béjaïa, 06000 Béjaïa, Algeria

Received: 5 May 2012 / Received in full form: 7 November 2012 / Accepted: 21 January 2013
Published online: 8 March 2013 –

Abstract. This paper aims to analyze the behavior of DC bipolar corona discharge in a two wires-to-plane configuration under variable humid air conditions. A circular biased probe was adapted to the plane and used to measure the ground-plane current density and electric field during the bipolar corona. The values of the electric field and the current density at the plane surface were the maximum beneath the two corona wires which decreased when moving away from them. The current-voltage characteristics followed the quadratic Townsend's law. The experimental results show that the bipolar corona discharge is strongly affected by the air humidity. The current density and the electric field decrease linearly with the humidity for all the tested wire diameters.

1 Introduction

In uniform fields when the field magnitude is increased gradually, just when measurable ionization begins, the ionization leads to a complete breakdown of the gap. However, in non-uniform fields, before the spark or breakdown between electrodes, there are many manifestations in the form of visual and audible discharges. These discharges are known as corona discharges and they are defined as a self-sustained electric discharge in which the field intensified ionization is localized only over a portion of the distance between the electrodes.

The stable corona discharge is used in various ways in an increasing number of engineering applications. The analysis of ionised fields in different geometrical electrode arrangements is an important area of research. One of the configurations mostly used for theoretical and experimental studies is the wire-to-plane geometry, which is largely used in the design of HVDC transmission line, electrostatic precipitators and separators [1–4], painting and spraying powders [5,6].

However, the corona effect produced by overhead HVDC transmission lines forms space-charges in the surrounding air which may, for example, cause radio interference, audible noise and electrification of objects, in addition to generating power losses. Also, the space-charges will affect the natural balance of ions in the air, which might have some unknown biological and environmental effects. Therefore, it is of interest to study the fields associated with HVDC power transmission lines in the presence of corona, both theoretically and experimentally.

Monopolar DC corona discharge consists of high-field active electrode surrounded by ionization region where free charges are produced, a low-field drift region where charged particles drift and a low-field electrode acting as a charge collector [7–9]. However, in bipolar DC corona discharge there are two high-field active electrodes each surrounded by an ionization region [10–13]. Figure 1 shows a simple bipolar DC wire-to-plane system. It consists of twin wires, each with a radius R, located at a height H above the ground plane and separated by a distance D. Assuming the wires to be infinitely long, the problem is considered two-dimensional in Cartesian coordinates. The space charge environment may be divided into two different regions: a bipolar region between the two conductors and a monopolar region between each wire and the ground. This discharge generates both positive and negative ions, and the pertinent recombination between ions of different polarity. This makes the analysis of a bipolar ionised field more complicated than that of a monopolar one. Also, the local value of the electric field strength depends not only on applied voltages and conductor geometry, but also on the generated space-charge.

The corona drift region is governed by the Poisson and current continuity equations. A complete solution of these equations is not straightforward. For practical applications, therefore, many authors have made some simplifying assumptions for the basic equations and empirical and semi empirical formulas have a useful function. Actually, the ions created in the ionization region drift to the passive electrode and the space charge modifies the original Laplacian applied field. Many theoretical and experimental works have been devoted to the study of the discharge behavior with various electrode systems. However,

[a] e-mail: yzebboudj@yahoo.fr

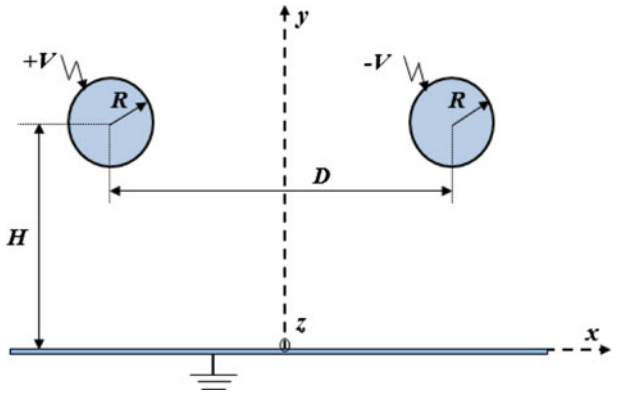

Fig. 1. Bipolar wire-to-plane configuration.

measurements of the modified electric field over the collector electrode are not easy in the presence of space charge.

In this paper we have proposed a method to measure the current density and electric field at the grounded plane where the humidity of ambient air is associated. The method uses the biased-current probe which was introduced by Tassicker [14] and further developed by many authors [15–17]. This type of probe can be miniaturized and is suitable for DC corona discharge investigations. A linear probe is used for current density and electric field measurements during the DC corona discharge in bipolar wires-to-plane [13] and wire-to-plane [17,18]. The probe collector is of rectangular form and surrounded by two plates biased at a voltage V_b. For the first time, we use the circular biased probe in the presence of space charge during the bipolar corona discharge.

2 Experimental method

2.1 Two wires to plane electrodes and air supply

This work aims to obtain new measurements of current density and electric field for the bipolar DC corona in two wires to plane system in which the humidity of the air is controlled. A plan view of the circular biased probe is shown in Figure 2. It is made up of a current collector (P) surrounded by a plane (E) with a guard plane (G). Twin wires (1), separated with a distance (D), are fixed with two insulating supports (2) at height (H) from the electrode (E) where the probe collector (P) is incorporated in the same level surface. All the components (E, G) are made of stainless steel and lay on insulating supports (3) which are placed on a grounded copper plate (4). The probe is also made of stainless steel and requires careful assembly. Indeed, some leakage current, of about a few pico-amperes affecting the current measurements, could originate from the bias plane or the high voltage wires. The probe collector (P) was fixed with two insulating plates (5) and the leakage was prevented by the copper plate (4). The leakage currents along the surfaces of the two insulating supports (2), affecting the current measurements, could originate from the high voltage wires. The leakage was prevented by using the guard planes (G).

Positive and negative direct voltage, supplied by a 0 to ±140 kV source (6), were applied simultaneously to the wires. The current collector (P) was connected to a pico-ammeter (7) and the bias plane (E) was connected online to the DC low voltage source (8). The electrode system and the measurement devices of temperature and humidity (9) were placed into a plexiglas box of 200 L (10), Figure 2c. The air inside this box came from the ambient atmosphere and was made to move in closed circulation by a pump (11). The humidity was controlled with a three-way circuit with taps. Air was hydrated (12) with the water vapor provided by heating a half full bottle of distilled water; ways (13) and (14) being closed. The drying of the air was made by the way (14) by using silicagel contained in a bottle, when the ways (12) and (13) were closed. The opening of way (13) and the closing of ways (12) and (14) of the circuit allow a constant humidity to be kept inside the box. Air was then filtered (15) before it was let in the box again. In order to eliminate the possible influence of the air flow on the corona discharge, the pump was stopped during the measurements.

2.2 Circular biased probe

The circular biased probe theory is fully developed in reference [14], but will be briefly summarized here. The probe collector (P) collects a current I_0 resulting from the corona discharge without the bias voltage in operation. This current reduces or increases to I when the voltage V_b is applied to the plane (E) and produces a bias field E_b. When the probe collector (P) is placed beneath the positive corona wire, E_b is opposed to the unknown field E at the surface of the probe when $V_\mathrm{b} < 0$ and E_b is added to E when $V_\mathrm{b} > 0$. On the other hand, when the probe collector is placed beneath the negative corona wire, E_b is added to E when $V_\mathrm{b} < 0$ and E_b is opposed E when $V_\mathrm{b} > 0$. The corona currents I under the condition V_b and I_0 under the condition $V_\mathrm{b} = 0$ are respectively:

$$I = JS = \mu\rho(E + E_\mathrm{b})S = \mu\rho \times \left(\frac{\varphi_{\mathrm{S}0} + \varphi_{\mathrm{S}1}}{\varepsilon_0}\right), \quad (1)$$

$$I_0 = J_0 S = \mu\rho E S = \mu\rho \times \frac{\varphi_{S0}}{\varepsilon_0}, \quad (2)$$

where μ is the positive ion mobility ($\mathrm{m}^2/\mathrm{V\ s}$), ρ is the space-charge density ($\mathrm{C/m}^3$), $S = \pi r_\mathrm{m}^2$ (m^2) is the effective surface of the collector (P), $r_\mathrm{m} = (r_\mathrm{e} + r)/2$ is the effective radius (see Fig. 2b), r is the radius of the collector (P), r_e is the radius of the plane orifice, $\varphi_{\mathrm{S}0}$ is the flux due to the unknown electric field E to be measured and $\varphi_{\mathrm{S}1}$ is the flux due to the biased electric field E_b:

$$\varphi_{\mathrm{S}0} = SE\varepsilon_0, \quad (3)$$

$$\varphi_{\mathrm{S}1} = C_0 V_\mathrm{b}, \quad (4)$$

where C_0 is the capacity between the probe collector (P) and the polarised plane (E) [14]:

$$C_0 = 4r\varepsilon_0 \left[1.07944 + 0.5 \ln\left(1 + \frac{r}{2g}\right)\right], \quad (5)$$

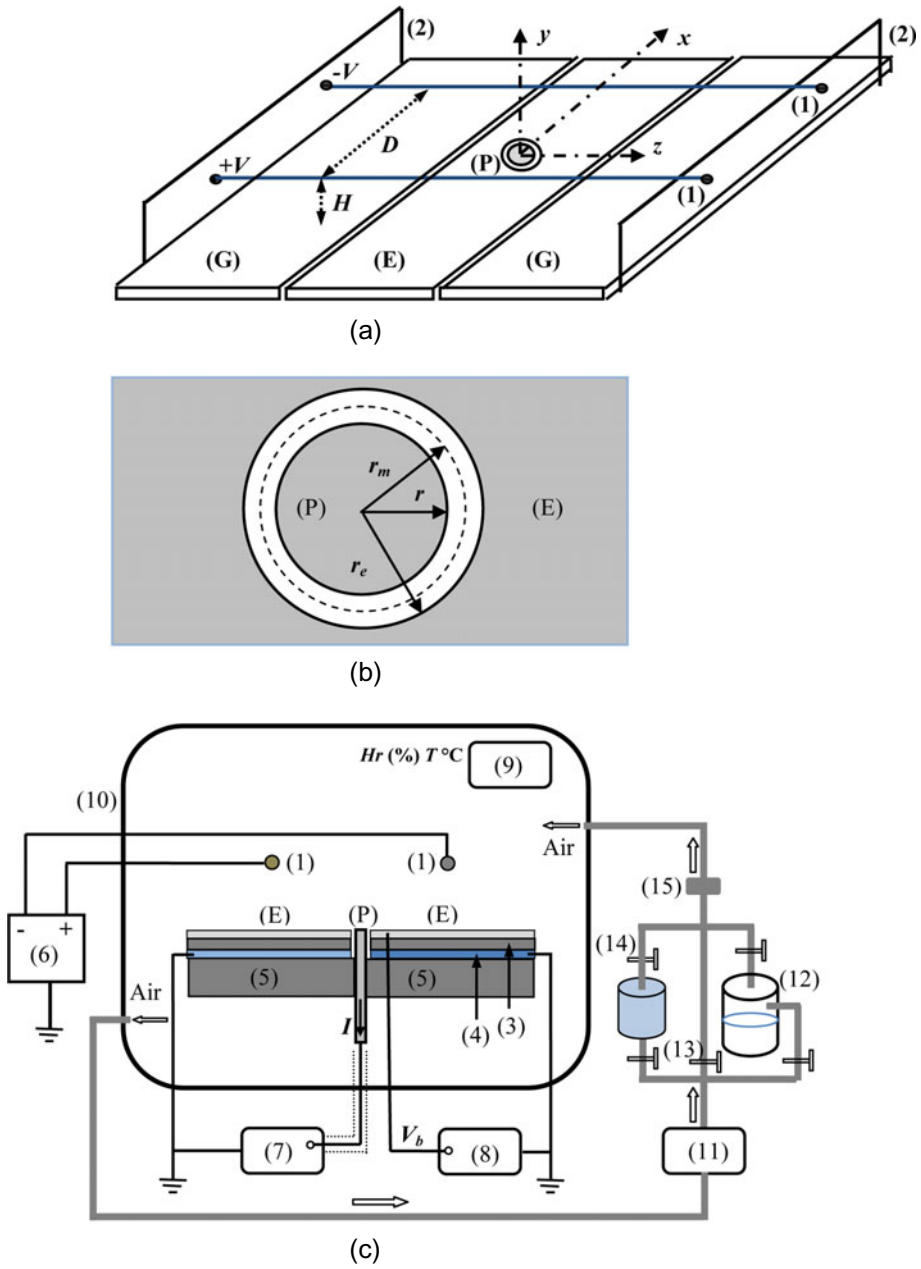

Fig. 2. Experimental assembly with the circular field probe (not in scale) (1) corona wires, (7) pico-ammeter, (11) pump, (2, 3, 5) insulating props, (8) DC low voltage source, (12) water vapor, (4) copper screen, (9) hygrometer, (14) silicagel, (6) DC high voltage source, (10) box, (15) filter, (P) probe collector, (E) biased electrode, (G) guard planes.

where $g = (r_e - r)$ is the air gap between (P) and (E).

From equations (1)–(4) the current ratio is given by:

$$\frac{I}{I_0} = 1 + \frac{C_0}{\pi\varepsilon_0 r_m^2}\frac{V_b}{E}. \quad (6)$$

The unknown external field E could be determined by the measurements of I_0 and I. The relationship (6) gives a characteristic I/I_0 linear with the biased voltage V_b. However, for high values of V_b, when the total field at the surface of the plane is inverted, due to the polarized electric field $E_b > E$, a deviation of the characteristics occurs and thus the relationship (6) is not valid.

The probe functions depend mainly on the choice of these dimensions and the precision of its construction. A good sensitivity of the current ratio I/I_0 is obtained for a probe radius r not very high and an air gap g very small as described by Selim and Waters [15] in their study of the probe properties. The authors indicate that the ratio r/g must be as high as reasonably possible. The probe must be easily removable for regular cleaning from dust. The model under consideration is optimized to obtain these qualities. The probe collector radius is $r = 2.235$ mm, the plane orifice is $r_e = 2.27$ mm, which gives an air gap $g = 0.035$ mm, a ratio $r/g = 64$, an effective radius of

the probe collector $r_m = r + g/2 = 2.2525$ mm and the capacity value $C_0 = 0.223$ pF.

Expression (6) can be written as:

$$\frac{I}{I_0} = 1 + PV_b, \tag{7}$$

with:

$$P = \frac{C_0}{\pi\varepsilon_0 r_m^2 E} = \frac{1585.35}{E}. \tag{8}$$

The slope P is determined by the measurements of the current ratio I/I_0 and the polarised voltage V_b, thus, the electric field E can be determined if P is known.

We made the measurements of I/I_0 for different bias voltages V_b, between -100 and $+100$ V, where the corona voltage $+V$ is applied to one wire and $-V$ is applied to the other simultaneously and the air humidity Hr is maintained a constant value during the tests. The measurements have allowed us to determine the field E, at the plane surface, using equations (7) and (8).

We also used the probe collector to measure the corona current-voltage characteristics I-V when the bias voltage $V_b = 0$. The corona voltage $+V$ and $-V$ are raised simultaneously and gradually from the value V_1 to the value V_2 such as $V_1 < V_i < V_2$, where V_i is the corona inception voltage. The measurements are made for two cases: when the probe collector is placed beneath the positive corona wire and when it is placed beneath the negative one.

3 Experimental results and discussion

The present work is concerned with the measurements of current density, electric field distributions at the plane surface and the corona current-voltage characteristics with a biased probe. The wires along the z-axis and the x-position of the probe collector on the passive electrode are achieved by displacing the wires (see Fig. 1). The measurements are carried out for various parameters such as:

- the applied voltage $V(+V$ and $-V)$;
- the x-position of the probe on the plane;
- the wire diameter $2R$;
- the relative humidity Hr.

The distance between the positive corona wire and the negative corona wire is fixed to $D = 120$ mm and the wire height is $H = 50$ mm. The tests are done within a large range of the corona voltage with varying humidity levels. The temperature and the pressure inside the box remain practically constant during the tests.

3.1 Current-voltage characteristics

In non-uniform field the interrelationship current-voltage of the corona discharge is the one described by Townsend [19]:

$$I = KV(V - V_i)(A/m), \tag{9}$$

where I is the corona current discharge, V is the applied voltage, V_i the inception corona voltage and K is the dimensional constant.

Other authors [20–22] have reported attempts to derive the Townsend's law for the point-to-plane system. The topical research on the corona current-voltage characteristic has reported attempts to elaborate a model for the Townsend's law in the point-to-plane where the dimension of the point radius is associated. Meng et al. [23] have recently introduced an empirical formula, based on the experimentation, for Townsend's law in the point-to-plane system:

$$I = K'V(V - V_i)^n, \tag{10}$$

where K' is the dimensional constant and n is the parameter which falls into the range 1.5–2.0 and takes a value of 1.6 for their study. The main criticism concerning Townsend's law suggested by the authors is that the parameters K' and V_0 both depend on the interelectrode distance. The current-voltage $I = f(V)$ characteristics are measured for the three tested wires and for various relative humidities. They follow the Townsend's law as shown in Figures 3–5.

- The measured I-V characteristics when the probe is placed beneath the negative corona wire are always upper to those measured beneath the positive one, Figure 3. In fact, the negative values of current are higher than the positive ones for the same applied voltage. This is due to the existence of a difference between the positive inception voltage and the negative one; also the mobility of the negative ions is higher than that of the positive ions.
- The relative humidity Hr affects the I-V characteristics. At a given applied voltage when Hr increases, the corona current decreases significantly. This can be

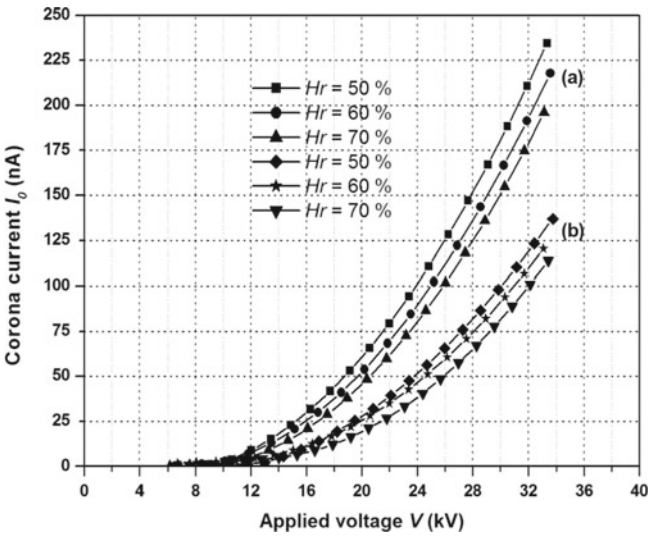

Fig. 3. Measured current-voltage characteristics for the $2R = 0.2$ mm diameter in various relative humidities: $T = 18$ °C, $P = 758$ mmHg (a) the probe collector beneath the negative wire; (b) the probe collector beneath the positive wire.

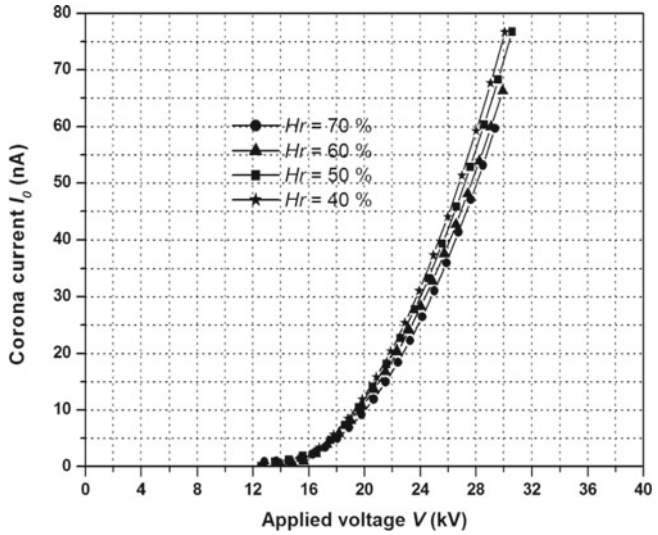

Fig. 4. Measured current-voltage characteristics for the $2R = 0.2$ mm diameter in various relative humidities and when the probe collector is placed beneath the positive wire: $T = 19$ °C; $P = 759$ mmHg.

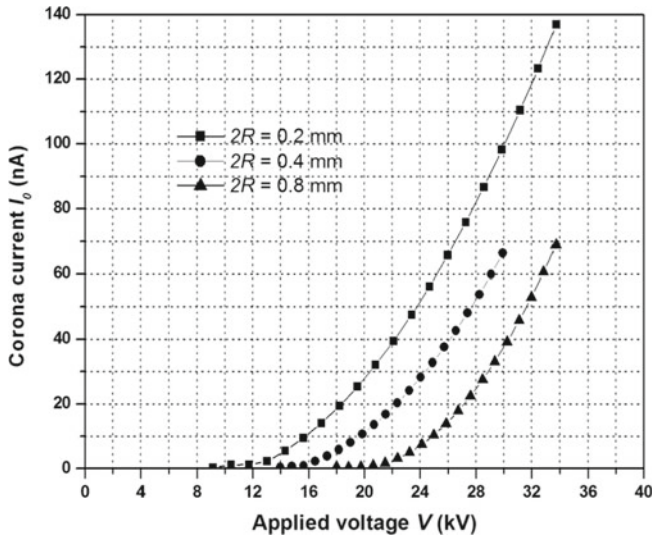

Fig. 5. Measured current-voltage characteristics for various wire diameters: $Hr = 70\%$; $T = 19$ °C; $P = 759$ mmHg.

explained by the electronegative nature of water vapor; adding water vapor to air would increase the attachment coefficient of the mixture, while the ionization coefficient would be constant. Furthermore, the ion mobility decreases with the humidity.

– The wire diameter $2R$ also affects the *I-V* characteristics. In fact, the inception voltage V_i increases when $2R$ increases as shown in Figure 5.

The *I-V* characteristics of the bipolar corona in wires-to-plane system appear to follow the general formula proposed by Meng et al. [23] given by equation (10). In our study the values of the exponent n for the wire radius experimented $2R$ are $n = 1.77$ for $2R = 0.2$ mm; $n = 1.63$ for $2R = 0.4$ mm and $n = 1.59$ for $2R = 0.8$ mm.

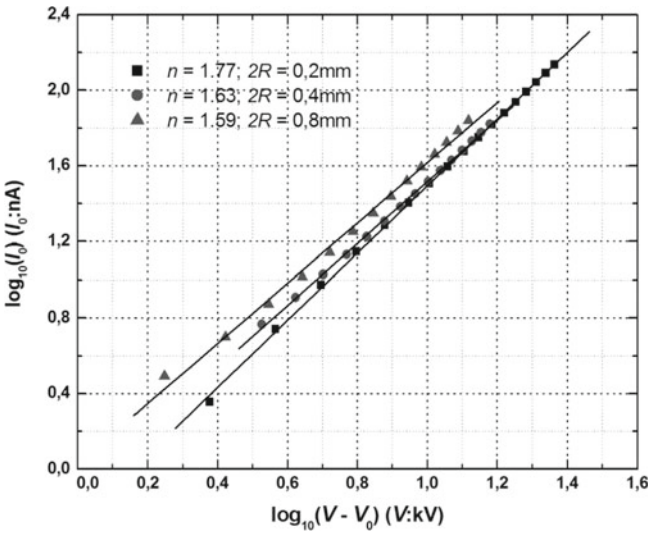

Fig. 6. The dependence of the corona current I_0 on the voltage difference $V - V_i$ for various wire diameters: $Hr = 70\%$; $T = 19$ °C; $P = 759$ mmHg.

Figure 6 shows the dependence of the corona current I_0 on the voltage difference $V - V_i$ (on a log scale).

3.2 Current density and electric field distributions on the passive electrode

The probe collector is used to measure the current density J_0 when the probe is unbiased ($V_b = 0$):

$$J_0 = \frac{I_0}{\pi r_m^2}, \tag{11}$$

where $r_m = 2.25$ mm is the effective radius of the probe collector and I_0 is the collected current of corona discharge. The measured current density and electric field profiles at the ground plane are shown in Figures 7 and 8, respectively. The measured values present a maximum beneath each wire (at $x = \pm D/2$) where the space-charge of the same polarity is concentrated and the wires-to-plane distance is minimal. It should be noted that in DC monopolar corona [18] where the probe collector is fixed at the center of the plane collector beneath the wire, the values of J and E are at a maximum for $x = 0$ and they decrease as we move away from the centre of this plane along the x-axis according to the Warburg's law [24]. For wire diameters of 0.200, 0.310, 0.400 and 0.800 mm the unique laws obtained by reference [18] from the curve-fitting are:

$$J(\theta) = J(0)\cos^4(\theta), \tag{12}$$

$$E(\theta) = E(0)\cos^{1.5}(\theta), \tag{13}$$

where:

$$\theta = \tan^{-1}(x/H). \tag{14}$$

In bipolar corona J and E are at a maximum beneath the wires and null at midway between the wires according to the superimposing principle. We have derived from

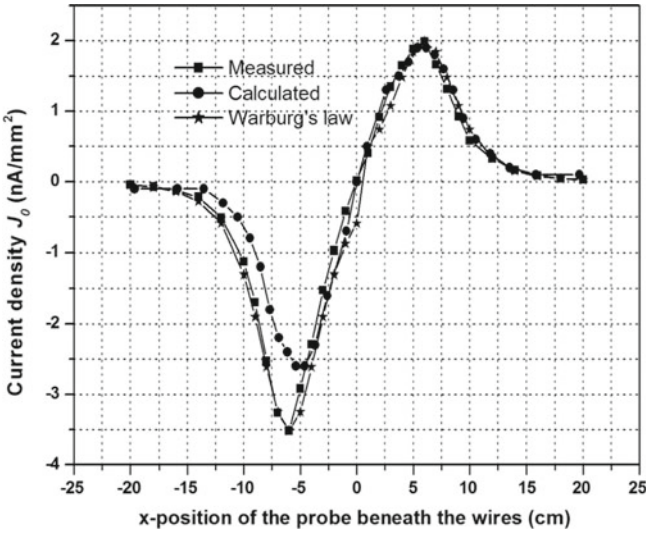

Fig. 7. Measured ground-plane current density for the applied voltage $V = 20$ kV; wire diameter $2R = 0.4$ mm: $Hr = 80\%$, $T = 22$ °C; $P = 760$ mmHg.

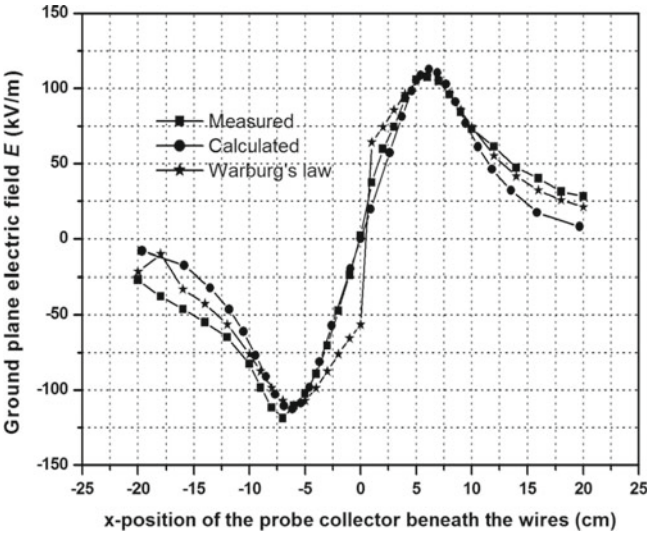

Fig. 8. Measured ground-plane electric field for the applied voltage V (kV); wire diameter $2R = 0.4$ mm; $Hr = 80\%$, $T = 22$ °C; $P = 760$ mmHg.

the curve-fitting for the current density J and the electric field E the Warburg's law respectively identical to equations (12) and (13). Moreover, the profiles are asymmetrical, that is, the negative values of the electric field and current density are higher than the positive ones for the same applied voltage. This is due to the existence of a difference between the positive inception voltage and the negative one; also the mobility of the negative ions is higher than that of the positive ions. The calculated current density and electric field at the ground plane using finite element method given by reference [13] are is shown in Figures 7 and 8. The calculated values predicted by this method are in good agreement with the measured values. The discrepancy observed between the two results can be attributed to experimental errors. In addition, measured

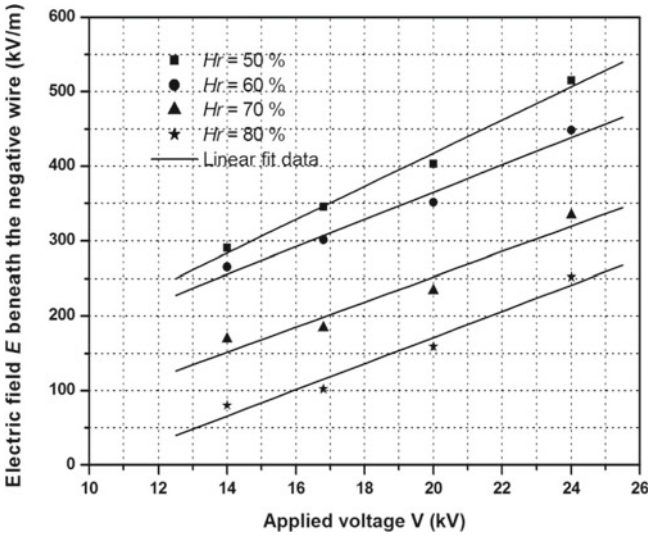

Fig. 9. Measured ground-plane electric field as a function of the applied voltage in various relative humidities Hr: the probe collector is placed beneath the negative wire $2R = 0.4$ mm diameter.

results vary markedly with changing atmospheric conditions.

The values of the electric field E at the ground plane with varying humidity and applied voltage are given in Tables 1 and 2. A summary of the test results are shown in Figure 9. The field E increases linearly with the applied voltage V at a given humidity Hr. At low voltage, E tends to the Laplacian field but breakdown at high applied voltage occurs when E is close to the propagation field: $E \approx 500$ kV/m necessary for positive streamer and E higher than this limit necessary for negative streamer. E increases also with the relative humidity Hr at a given applied voltage V.

4 Conclusion

Measurements of the current density and electric field using a bias probe at the ground plane in DC bipolar corona system with varying humidity are presented in this paper. The current dependence upon voltage follows a common square law $I = kV(V - V_i)$ of Townsend. It is significantly reduced by increasing humidity and at a given voltage the negative value of the current is always higher than that of the positive one.

The measured current density J and electric field E distributions at the ground plane are similar to those originally proposed by Warburg according to the superimposing principle of the two polarities, but the profiles are asymmetrical, that is, the negative values of electric field and current density are higher than the positive ones for the same applied voltage. It is indeed possible to interpret this result by the existence of a difference between the positive inception voltage and the negative one, and a difference between the mobility of the positive ions and the negative ones.

Table 1. Results of electric field measurement at the ground plane with the twin wires of diameters $2R = 0.4$ mm.

Electric field measurement at the ground plane E (kV/m)				
Probe collector beneath the **negative** corona wire ($x = -6$ cm)				
V (kV)	14	16.8	20	24
Hr (%)				
50 ± 5	**291** ± 14.6	**345** ± 17.3	**403** ± 20.2	**515** ± 25.8
60 ± 6	**265** ± 13.3	**301** ± 15.1	**351** ± 17.6	**448** ± 22.4
70 ± 7	**169** ± 8.5	**184** ± 9.2	**234** ± 11.7	**334** ± 16.7
80 ± 8	**80** ± 4.0	**102** ± 5.1	**159** ± 8.0	**252** ± 12.6
Probe collector beneath the **positive** corona wire ($x = +6$ cm)				
V (kV)	**14**	**16.8**	**18**	**20**	**24**
Hr (%)				
50± 5	**69** ± 3.5	**173** ± 8.7	**217**± 10.9	**296**± 14.8	**342**± 17.1
60 ± 6	**36** ± 1.8	**127**± 6.4	**158** ± 7.9	**236** ± 11.8	**297** ± 14.9
70 ± 7	**20** ± 1.0	**68** ± 3.4	**93** ± 4.7	**151** ± 7.6	**228** ± 11.4
80 ± 8	**6** ± 0.3	**23** ± 1.15	**43** ± 2.15	**89** ± **4.5**	**177** ± 8.9
$2R = 0.2$ mm; $T = 19$ °C; $P = 759$ mmHg					

Table 2. Results of electric field measurement at the ground plane with the twin wires of diameters $2R = 0.8$ mm.

Electric field measurement at the ground plane E (kV/m)				
Probe collector beneath the **negative** corona wire ($x = -6$ cm)				
V (kV)	**24**	**26**	**28**	**30**
Hr (%)				
40 ± 4	**390** ± 19.5	**473** ± 23.7	**541** ± 27.1	**642** ± 32.1
50 ± 5	**362** ± 18.1	**436** ± 21.8	**536** ± 26.8	**610** ± 30.5
60 ± 6	**301** ± 15.1	**377** ± 18.9	**491** ± 24.6	**574** ± 28.7
70 ± 7	**180** ± 9.0	**262** ± 13.1	**431** ± 21.6	**543** ± 27.2
Probe collector beneath the **positive** corona wire ($x = +6$ cm)				
V (kV)	**24**	**26**	**28**	**30**
Hr (%)				
50 ± 5	**350**± 17.5	**391** ± 19.6	**461** ± 23.1	**499** ± 25.0
60 ± 6	**275** ± 13.8	**338** ±1.9	**385** ± 19.6	**425** ± 21.6
70 ± 7	**145** ± 7.3	**209** ± 10.5	**251** ± 12.6	**279** ± 14.0
80 ± 8	**34** ± 1.7	**104** ± 5.2	**139** ± 7.0	**167** ± 8.4
$2R = 0.8$ mm; $T = 19$ °C; $P = 759$ mmHg				

The measurements show that the electric field E at the plane varies linearly with the applied voltage V and it decreases significantly when the humidity increases. The field E under the negative wire is higher than the field under the positive one.

References

1. A. Mizuno, IEEE Trans. Dielectr. Electr. Insul. **7**, 615 (2000)
2. H. Nouri, N. Zouzou, E. Moreau, L. Dascalescu, Y. Zebboudj, J. Electrostat. **70**, 20 (2012)
3. J.S. Chang, J. Electrostat. **57**, 273 (2003)
4. J. Podlinski, J. Dekowski, J. Mizeraczyk, D. Brocilo, J.S. Chang, J. Electrostat. **64**, 259 (2006)
5. Q. Ye, T. Steigleder, A. Scheibe, J. Domnick, J. Electrostat. **54**, 189 (2002)
6. A.A. Elmoursi, IEEE Trans. Ind. Appl. **28**, 1174 (1992)
7. J.E. Jones, J. Dupuy, G.O.S. Schreiber, R.T. Waters, J. Phys. D: Appl. Phys. **21**, 322 (1988)
8. Y. Zebboudj, G. Hartmann, Eur. Phys. J. Appl. Phys. **7**, 167 (1999)
9. Y. Zebboudj, R. Iken, Eur. Phys. J. Appl. Phys. **10**, 211 (2000)
10. Z.M. Al-Hamouz, IEEE Trans. Ind. Appl. **32**, 1266 (1996)
11. G.P. Reichel, J.M. Mäkelä, R. Karch, J. Necid, J. Aerosol Sci. **27**, 931 (1996)
12. U. Corbellini, P. Pelachi, IEEE Trans. Power Deliv. **11**, 3 (1996)
13. A. Kasdi, Y. Zebboudj, H. Yala, Eur. Phys. J. Appl. Phys. **37**, 323 (2007)
14. O.J. Tassicker, Proc. IEE **121**, 213 (1974)
15. E.O. Selim, R.T. Waters, IEEE Trans. **16**, 458 (1980)
16. A. Bouziane, G. Hartmann, K. Hidaka, M.C. Taplamacioglu, R.T. Waters, IEE Proc.: Sci. Meas. Technol. **141**, 111 (1994)

17. Y. Zebboudj, R. Ikene, G. Hartmann, Eur. Phys. J. Appl. Phys. **6**, 195 (1999)
18. N. Oussalah, Y. Zebboudj, Eur. Phys. J. Appl. Phys. **34**, 215 (2006)
19. J.S. Townsend, *Electricity in Gases* (Oxford University Press, UK, 1915), pp. 375–376
20. B.L. Henson, J. Appl. Phys. **52**, 709 (1981)
21. K. Yamada, J. Appl. Phys. **96**, 2472 (2004)
22. G.F. Ferreira, O.N. Oliveira, J.A. Giacometti, J. Appl. Phys. **59**, 3045 (1986)
23. X. Meng, H. Zhang, J. Zhu, J. Phys. D: Appl. Phys. **41**, 065209 (2008)
24. E. Warburg, *Handbuch der Physik*, vol. 14 (Springer, Berlin, 1927), pp. 154–155